Microchimica Acta (2019) 186: 378
https://doi.org/10.1007/s00604-019-3495-5

ORIGINAL PAPER

Golf ball-like MoS_2 nanosheet arrays anchored onto carbon nanofibers for electrochemical detection of dopamine

Hong Yan Yue[1] · Peng Fei Wu[1] · Shuo Huang[1,2] · Zeng Ze Wang[1] · Xin Gao[1] · Shan Shan Song[1] · Wan Qiu Wang[1] · Hong Jie Zhang[1] · Xin Rui Guo[1]

Received: 4 January 2019 / Accepted: 12 May 2019 / Published online: 27 May 2019

Abstract

Arrays of molybdenum(IV) disulfide nanosheets resembling the shape of golf balls (MoS_2 NSBs) were deposited on carbon nanofibers (CNFs), which are shown to enable superior electrochemical detection of dopamine without any interference by uric acid. The MoS_2 NSBs have a diameter of ~ 2 μm and are made up of numerous bent nanosheets. MoS_2 NSBs are connected by the CNFs through the center of the balls. Figures of merit for the resulting electrode include (a) a sensitivity of 6.24 $\mu A \cdot \mu M^{-1} \cdot cm^{-2}$, (b) a low working voltage (+0.17 V vs. Ag/AgCl), and (c) a low limit of detection (36 nM at $S/N = 3$). The electrode is selective over uric acid, reproducible and stable. It was applied to the determination of dopamine in spiked urine samples. The recoveries at levels of 10, 20 and 40 μM of DA are 101.6, 99.8 and 107.8%.

Keywords MoS_2 nanosheet · Carbon nanofibers · Dopamine · Uric acid · Hydrothermal synthesis · Electroanalysis

Introduction

Dopamine (DA) is a well-known neurotransmitter, which plays an extremely important role in the central nervous system, kidney and cardiovascular system [1, 2]. Some neuropsychiatric diseases are related with it [3, 4]. Therefore, it is vitally important to determine DA for the diagnosis and treatment of these diseases. Many methods have been reported for the detection of DA, such as electrochemical method, chemiluminescence, capillary electrophoresis, spectrophotometry, and flow injection [5–11]. Among them, the electrochemical methods have the advantages of simple operation, high selectivity and sensitivity, fast response and low cost [12], Some new nanomaterials modified electrodes have been used for electrochemical detection of DA [13–17]. However, these modified electrodes have some shortcomings, such as low sensitivity and high detection limit. How to improve the sensitivity of the modified electrodes is the focus of current researchers.

Carbon nanofibers (CNFs), an interesting one-dimensional carbon material, are widely used in solar cells, supercapacitors and nanoprobes [18–20]. CNFs have unique nanofiber network structure, good conductivity, chemical stability and biocompatibility, and they are ideal candidate materials for high-performance nanoprobes [21]. However, CNFs have a small specific surface area and a small number of active sites, resulting in lower sensitivity in actual detection [22]. The nanofiber network structure of CNFs is an ideal carrier for combining with other materials, which will further enhance the electrochemical properties.

Molybdenum disulfide (MoS_2) is a layered compound with graphene-like structure, which has attracted a wide attention and has been widely used in various fields [23–25]. In order to further enhance its physical and chemical properties, considerable efforts have been made to prepare MoS_2 nanomaterials with different morphologies. Among them, MoS_2 nanosheet balls (MoS_2 NSBs) composed of numerous nanosheets have high surface ratio, catalytic efficiency, porous surface, biocompatibility and chemical stability, which are considered as excellent materials for nanoprobes [26–28].

Electronic supplementary material The online version of this article (https://doi.org/10.1007/s00604-019-3495-5) contains supplementary material, which is available to authorized users.

✉ Hong Yan Yue
hyyue@hrbust.edu.cn

[1] School of Materials Science and Engineering, Harbin University of Science and Technology, Harbin 150040, People's Republic of China

[2] Department of Neurology, The First Affiliated Hospital of Harbin Medical University, Harbin 150001, People's Republic of China

Here, a novel golf ball-like MoS_2 NSBs were successfully grown on the CNFs. The hybrid MoS_2 NSB/CNFs was used for electrochemical determination of DA under the interference of uric acid (UA). Due to the synergistic effect of MoS_2 NSBs with large specific surface area and CNFs with high conductivity, the hybrid shows a high sensitivity, low LOD, good selectivity, reproducibility and stability for the determination of DA. It is expected to be used in practical DA detection.

Experimental

Preparation of the molybdenum(IV) disulfide nanosheet balls (MoS_2 NSBs) on carbon nanofibers (CNFs)

CNFs were synthesized by electrospinning, which is same as previously reported [29]. The prepared CNFs were cut into a size of 1 cm × 2 cm and put in concentrated nitric acid (Sinopharm Chemical Reagent Co., Ltd. China http://www.reagent.com.cn/) for 18 h to prepare the activated CNFs. Then, sodium molybdate ($Na_2MoO_4{\cdot}2H_2O$, 0.5 mmol) and thiourea (CH_4N_2S, 2.5 mmol) (Sinopharm Chemical Reagent Co., Ltd. China http://www.reagent.com.cn/) were added to 0.075 L deionized water (Sichuan Wortel Water Treatment Equipment Co., Ltd. China http://www.sc-woter.com/) and stirred for 20 mins to prepare hydrothermal solution. The activated CNFs and hydrothermal solution were transferred to a 0.1 L Teflon-lined stainless-steel autoclave and heated at 220 °C for 22 h, and then cooled to ambient temperature. Finally, the samples were washed with deionized water and dried in a vacuum freeze dryer for 1 h to obtain MoS_2 NSB/CNFs. All the chemical reagents in this experiment are analytical reagents.

Characterizations

The morphologies of CNFs and MoS_2 NSB/CNFs were characterized by JSM7000F scanning electron microscope (SEM). X-ray diffraction (XRD) experiments were recorded by Rigaku Ratoflex D/MAX diffractometer.

Electrochemical measurements

All electrochemical measurements were conducted on a VMP3 electrochemical workstation (Biologic Science Instrument, France). The electrochemical measurements include cyclic voltammetry (CV), differential pulse voltammetry (DPV), electrochemical impedance spectroscopy (EIS) and amperometric responses. MoS_2 NSB/CNFs electrode was used as the working electrode, Ag/AgCl as the reference electrode and platinum wire as the counter electrode. The effective plane area of the MoS_2 NSB/CNFs electrode was 0.7 cm^2. The specific parameters of electrochemical measurements are the same as those reported previously [30].

Results and discussion

Preparation and characterizations of the MoS_2 NSB/CNFs

Figure 1 shows the preparation process schematic of MoS_2 NSB/CNFs and electrochemical redox reactions of DA and

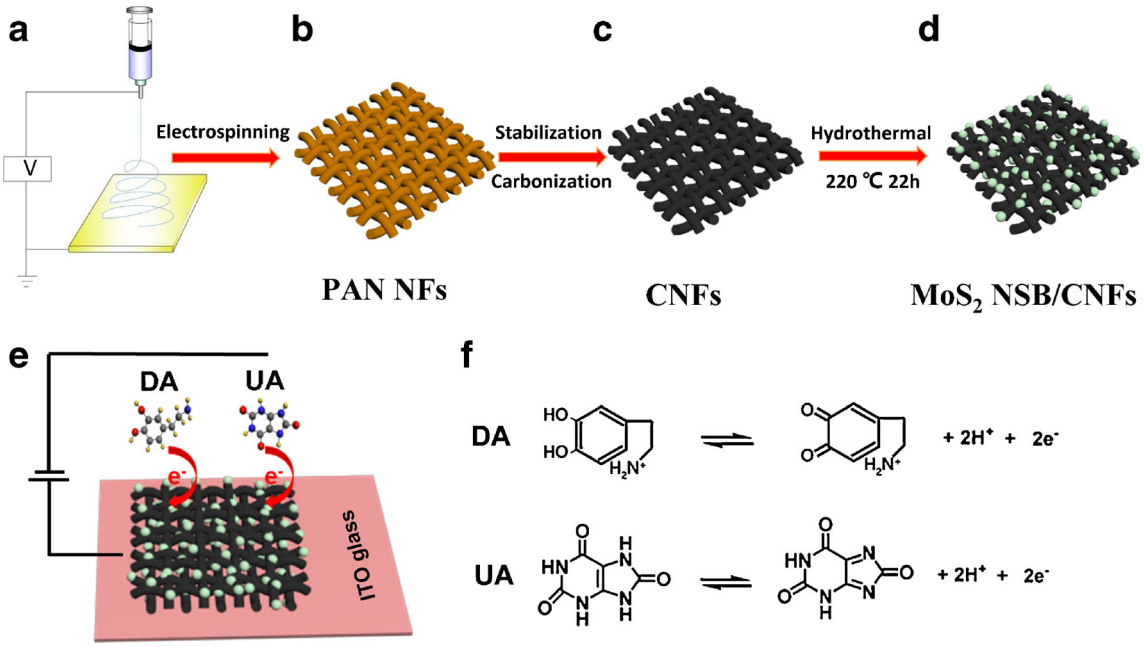

Fig. 1 | Schematic of preparation process of the MoS_2 NSB/CNFs and electrochemical redox reactions of DA and UA at the electrode

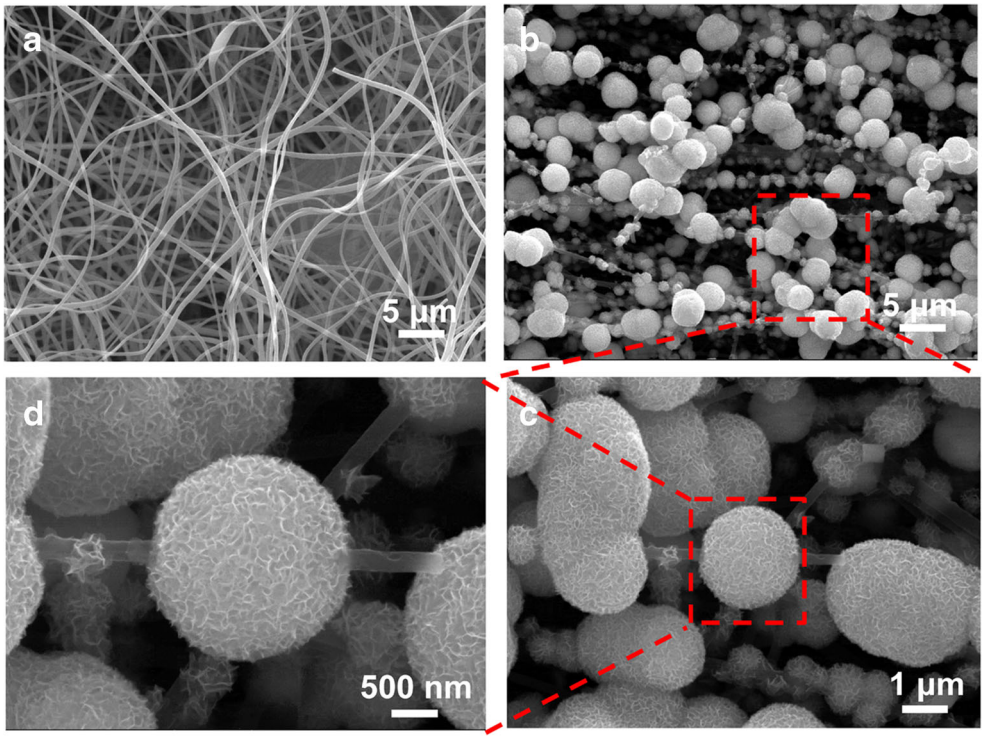

Fig. 2 | SEM images of CNFs and MoS_2 NSB/CNFs. **a,** CNFs. **b-d,** MoS_2 NSB/CNFs with different magnifications

UA at the MoS_2 NSB/CNFs electrode. First, the polyacrylonitrile nanofibers (PAN NFs) were prepared by electrospinning (Fig. 1a-b). Then, PAN NFs were stabilized at 300 °C and carbonized at 900 °C to obtain CNFs (Fig. 1c). After that, CNFs were placed in hydrothermal solution and heated at 220 °C for 22 h to prepare MoS_2 NSB/CNFs (Fig. 1d). The electrochemical redox reactions of DA and UA occurs on the surface of MoS_2 NSB/CNFs (Fig. 1e-f).

Figure 2 shows the SEM morphologies of CNFs and MoS_2 NSB/CNFs. The CNFs are interwoven into a network structure, whose average diameter is ~ 200 nm (Fig. 2a). After hydrothermal reaction, discontinuous MoS_2 NSBs were grown on the CNFs (Fig. 2b). By observing SEM images with high-magnification, MoS_2 NSBs with the diameter of ~ 2 μm are made up of nemerous bent nanosheets to form a porous structure and CNFs connect them through the center of the ball (Fig. 2c-d), which further increases the adsorption sites of biological molecules. XRD image of MoS_2 NSB/CNFs clearly shows the diffraction peaks of CNFs and MoS_2 NSB (Fig. S1). All above results indicate that golf ball-liked MoS_2 NSB/CNFs is synthesized successfully.

Electrochemical properties

Figure 3 shows the CV curves of MoS_2 NSB/CNFs electrode in 0.1 mM DA and UA at a scan rate of 100 mV s^{-1}. The

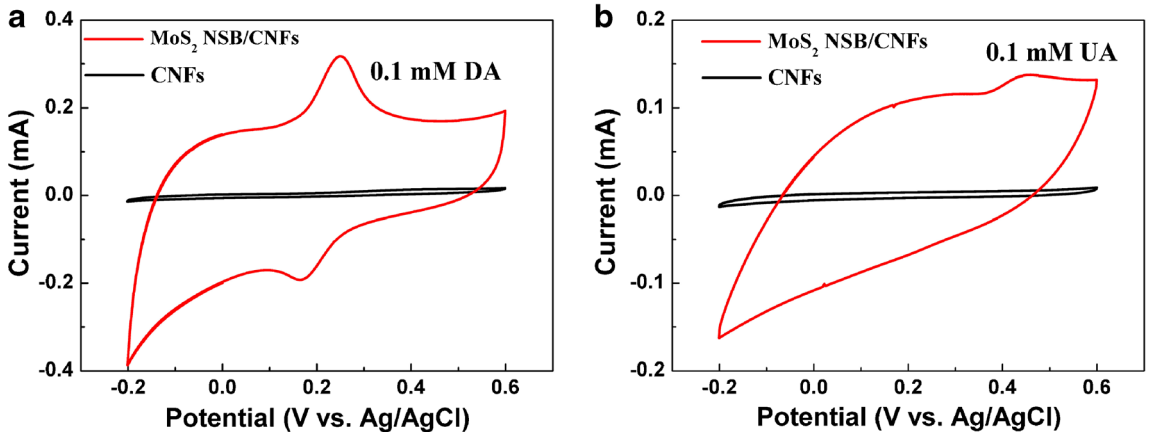

Fig. 3 | CV curves of CNFs and MoS_2 NSB/CNFs in 0.1 mM DA and UA at a scan rate of 100 mV s^{-1}. **a,** DA. **b,** UA. The oxidation peak potential for LD and UA appears at ~ 0.25 and 0.45 V, respectively

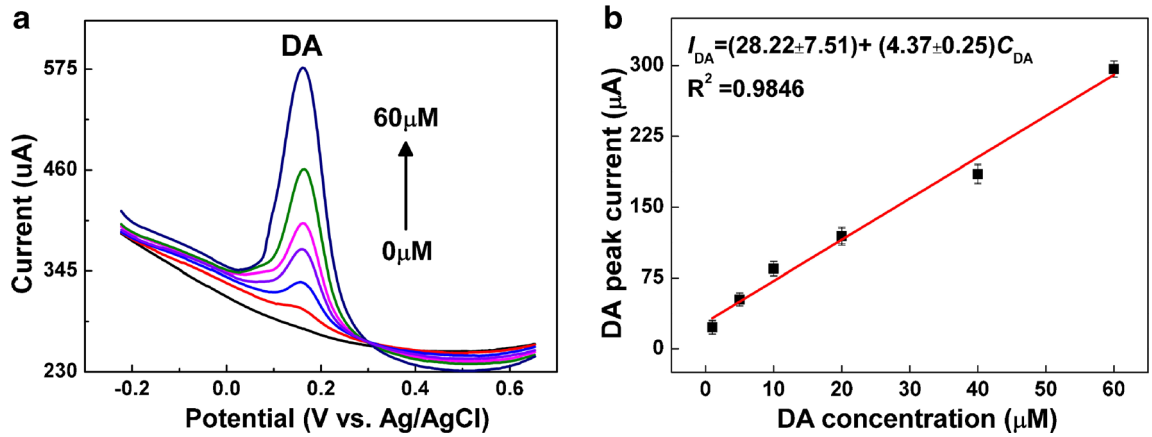

Fig. 4 Differential pulse voltammetric (DPV) curves of MoS_2 NSB/CNFs electrode in DA with different concentrations. **a**, The DA concentration from bottom to top is 0, 1, 5, 10, 20, 40 and 60 μM. **b**, Relationship of the DA oxidation peak current vs. concentration. DPV conditions: pulse height is 50 mV, pulse width is 0.2 s, step height is 4 mV and step time is 0.5 s

results show that the DA and UA oxidation peaks of MoS_2 NSB/CNFs electrode are significantly higher than those of bare CNFs electrode. This may be the synergistic effect of MoS_2 NSBs with large specific surface area and abundant active sites, and CNFs with high conductivity. The calculated ECSA of the MoS_2 NSB/CNFs electrode is 3.9 cm^2 (Fig. S2a). The charge transfer resistance of CNFs and MoS_2 NSB/CNFs is 380 and ~ 10 Ω (Fig. S2b). The results show that the conductivity of CNFs can be significantly improved by combination of MoS_2 NSBs. Moreover, this indicates that DA and UA are both adsorption control processes of MoS_2 NSB/CNFs at the scanning range of 10–100 $mV{\cdot}s^{-1}$ (Fig. S3).

DPV has a higher current sensitivity than CV, so DPV technology is used for the determination of DA [31]. Figure 4 depicts the DPV curves of MoS_2 NSB/CNFs electrodes in DA solution with different concentrations. The linear

Table 1 Summary of the previously published results for individual detection of DA by DPV using different electrodes

Electrodes	LDR (μM)	LOD (μM) (S/*N* = 3)	Sensitivity ($\mu A{\cdot}\mu M^{-1}{\cdot}cm^{-2}$)	Method	Ref.
CuO/CN-5/GCE	0.2–16	0.06	0.83	DPV	[32]
	16–78.7		0.33		
AgNC@PDA-NS/CFG/GE	2.5–130	0.25	0.54	DPV	[33]
Au/CoS_2/IL-GN/GCE	0.1–400	0.04	0.61	DPV	[34]
GO-ZIF67	02–80	0.05	1.39	DPV	[35]
NP-PtY/GR/GCE	0.9–82	0.36	5.86	DPV	[36]
GCE/P-Arg/ErGO/AuNP	1–50	0.001	2.48	DPV	[37]
NPG-μE	0.1–10	0.03	–	SWV	[38]
RGO-CdSe QD/GCE	4.9–74	0.11	0.16	DPV	[39]
MoS_2 NSB/CNFs	**1–60**	**0.04**	**6.24**	**DPV**	**Ours**

LDR: linear dynamic range. LOD: limit of detection. SWV: square wave voltammetry

CuO/CN-5: CuO and g-C_3N_4 modified glassy carbon electrode

AgNC@PDA-NS/CFG/GE: gold electrode modified with carboxyl-functionalized graphene and silver nanocube functionalized DA nanospheres

Au/CoS_2/IL-GN/GCE: gold nanoparticles/CoS_2/ionic liquid-graphene oxide nanosheets modified glassy carbon electrode

GO-ZIF67: Co(II)-based zeolitic imidazolate framework and graphene oxide electrode

NP-PtY/GR/GCE: nanoporous platinum-yttrium alloy/graphene modified glassy carbon electrode

GCE/P-Arg/ErGO/AuNP: glassy carbon electrode modified with poly(L-arginine), reduced graphene oxide and gold nanopar

NPG-μE: nanoporous gold-gold microelectrode

RGO-CdSe QD/GCE: reduced graphene oxide which decorated thioglycolic acid capped cadmium selenide quantum dots

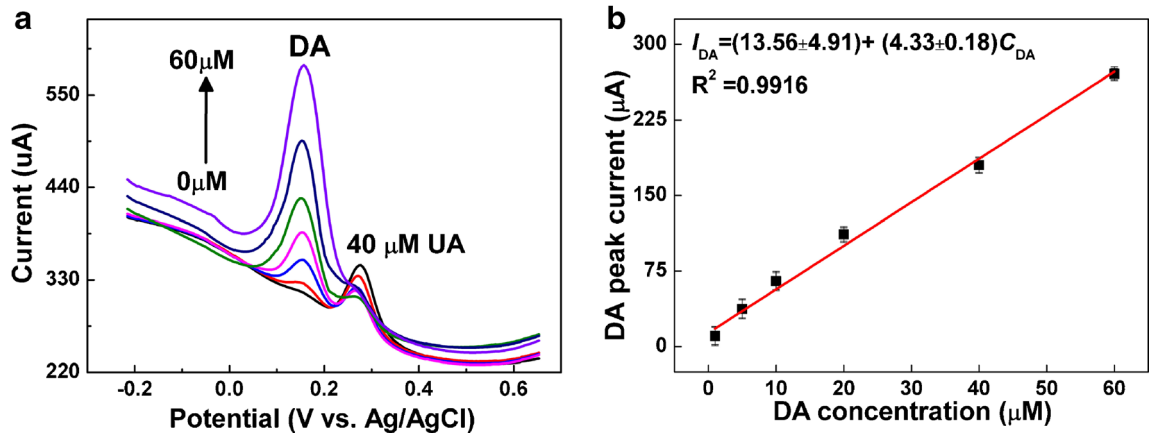

Fig. 5 DPV curves of MoS_2 NSB/CNFs electrode in DA with different concentrations in the presence of 40 μM UA. **a,** The DA concentrations from bottom to top is 0, 1, 5, 10, 20, 40 and 60 μM. **b**, Relationship of the DA oxidation peak current vs. concentration. The DPV conditions are the same as in Fig. 4

fitting equation is $I_{DA} = (28.22 \pm 7.51) + (4.37 \pm 0.25)C_{DA}$ ($R^2 = 0.9846$) indicates the linear relationship between the oxidation peak current of DA and its concentration. Hence, the sensitivity of the MoS_2 NSB/CNFs electrode for detecting DA is 6.24 $\mu A \cdot \mu M^{-1} \cdot cm^{-2}$. The LOD of the MoS_2 NSB/CNFs electrode is obtained using the formula: $LOD = 3S_b/m$, where m is the slope of the fitting curve (4.37 $\mu A \cdot \mu M^{-1}$), S_b is the standard deviation of the blank signal (Fig. S4), so the LOD is 0.036 μM. The sensitivity and LOD are superior than those of the previous reported (Table 1) [32–39].

Since UA and DA coexist in human body fluid, it is necessary to investigate the interference of UA on the detection of DA. Figure 5 depicts the DPV curves of MoS_2 NSB/CNFs electrode in mixtures of DA and UA. The concentration of DA (C_{DA}) and its oxidation current (I_{LD}) is linearly correlated, and the linear equation is $I_{DA} = (13.56 \pm 4.91) + (4.33 \pm 0.18)C_{DA}$ ($R^2 = 0.9916$). The result shows that the presence of UA has no significant influence on the detection of DA.

The selectivity of the MoS_2 NSB/CNFs electrode for DA detection was investigated by continuous injection of potentially interfering ions, such as uric acid, ascorbic acid, folic acid, KCl, Na_2SO_4, NaCl, $NaNO_3$ and NaOH, as shown in Fig. S5. There is no current response when adding interfering substances, which confirms that the MoS_2 NSB/CNFs electrode has a good selectivity performance.

However, DA cannot be detected precisely when it coexists with neurotransmitters, such as, levodopa (LD), norepinephrine (NE) and epinephrine (E) due to the same oxidation potential.

Reproducibility and stability

To analyze the repeatability and stability of MoS_2 NSB/CNFs electrode, 10 μM DA was tested multiple times with DPV. After repeating 9 measurements every 10 min at room temperature, the relative standard deviations (RSD) was 1.9% (Fig. S6a), indicating that the MoS_2 NSB/CNFs electrode had a good reproducibility. The MoS_2 NSB/CNFs electrode was placed in a 0.01 M phosphate buffered saline and the DPV test was performed in 10 μM DA every 2 days. After 14 days, the oxidation peak current of DA decreased by 7.1% (Fig. S6b), indicating that the MoS_2 NSB/CNFs electrode had an excellent stability.

Real sample analysis

The feasibility of the MoS_2 NSB/CNFs electrode was investigated by the detection of human urine samples. The experimental results obtained are shown in ESM. The recoveries of the detection of 10, 20 and 40 μM DA are 101.6, 99.8 and 107.8%. The RSD is 1.9, 2.2 and 1.7%, respectively. The results show that MoS_2 NSB/CNFs electrodes can be used for real urine test and have a great potential for clinical applications.

Conclusions

A novel MoS_2 NSB/CNFs hybrid was prepared by combining electrospinning preparation of CNFs and in-situ growth of MoS_2 NSBs on the surface of CNFs. The golf ball-like MoS_2 NSBs are made up of numerous bent nanosheets and CNFs connect them through the center of the ball. The MoS_2 NSB/CNFs electrode exhibits excellent electrochemical properties for the detection of DA due to the synergistic effect of the two nanomaterials. It is also expected to be used for clinical determination of DA.

Acknowledgements This work is supported by the fundamental research foundation for University of Heilongjiang province (LGYC2018JQ012) and the Innovative Talent Fund of Harbin city (2016RAQXJ185).

Compliance with ethical standards The authors declare that they have no competing interests.

References

1. Raj M, Gupta P, Goyal RN, Shim YB (2017) Graphene/conducting polymer nano-composite loaded screen printed carbon sensor for simultaneous determination of dopamine and 5-hydroxytryptamine. Sensors Actuators B Chem 239:993–1002
2. Yang H, Zhao X, Chang H, Xing R, Yang JH, Liu S, Liu X (2018) Sensitive determination of dopamine and paracetamol based on carbon nanotubes-supported Pd nanoparticles. J Nanosci Nanotechnol 18:500–509
3. Yan X, Gu Y, Li C, Tang L, Zheng B, Li Y, Zhang Z, Yang M (2016) Synergetic catalysis based on the proline tailed metalloporphyrin with graphene sheet as efficient mimetic enzyme for ultrasensitive electrochemical detection of dopamine. Biosens Bioelectron 77:1032–1038
4. Bagheri H, Pajooheshpour N, Jamali B, Amidi S, Hajian A, Khoshsafar H (2017) A novel electrochemical platform for sensitive and simultaneous determination of dopamine, uric acid and ascorbic acid based on Fe_3O_4-SnO_2-Gr ternary nanocomposite. Microchem J 131:120–129
5. Yurong W, Hengwu C (2005) Integrated capillary electrophoresis amperometric detection microchip with replaceable microdisk working electrode. II. Influence of channel cross-sectional area on the separation and detection of dopamine and catechol. J Chromatogr A 1080:192–198
6. Yu J, Ge L, Huang J, Wang S, Ge S (2011) Microfluidic paper-based chemiluminescence biosensor for simultaneous determination of glucose and uric acid. Lab Chip 11:1286–1291
7. Prasad BB, Tiwari K, Singh M, Sharma PS, Patel AK, Srivastava S (2008) Molecularly imprinted polymer-based solid-phase microextraction fiber coupled with molecularly imprinted polymer-based sensor for ultratrace analysis of ascorbic acid. J Chromatogr A 1198:59–66
8. Wang HY, Qiu SH, Li XX, Ji GJ, Yue S (2003) Fluorimetric determination of dopamine in pharmaceutical products and urine using ethylene diamine as the fluorigenic reagent. Anal Chim Acta 497: 93–99
9. Baron R, Zayats M, Willner I (2005) Dopamine-, L-DOPA-, adrenaline-, and noradrenaline-induced growth of Au nanoparticles: assays for the detection of neurotransmitters and of tyrosinase activity. Anal Chem 77:1566–1571
10. Satyanarayana M, Koteshwara Reddy K, Vengatajalabathy Gobi K (2015) Nanobiocomposite based electrochemical sensor for sensitive determination of serotonin in presence of dopamine, ascorbic acid and uric acid in vitro. Electroanalysis 26:2365–2372
11. Sanghavi BJ, Wolfbeis OS, Hirsch T, Swami NS (2015) Nanomaterial-based electrochemical sensing of neurological drugs and neurotransmitters. Microchim Acta 182:1–41
12. Vellaichamy B, Periakaruppan P, Paulmony T (2017) Evaluation of a new biosensor based on in situ synthesized PPy-ag-PVP nanohybrid for selective detection of dopamine. J Phys Chem B 121:1118–1127
13. Song X, Fu J, Wang J, Li C, Liu Z (2018) Simultaneous voltammetric determination of acetaminophen and dopamine using a glassy carbon electrode modified with copper porphyrin-exfoliated graphene. Microchim Acta 185(8):369–377
14. Dai H, Chen D, Li Y, Cao P, Wang N, Lin M (2018) Voltammetric sensing of dopamine based on a nanoneedle array consisting of $NiCo_2S_4$ hollow core-shells on a nickel foam. Microchim Acta 185(3):157–163
15. Hou Y, Sheng K, Lu Y, Ma C, Liu W, Men X, Xu L, Yin S, Dong B, Bai X, Song H (2018) Three-dimensional graphene oxide foams loaded with AuPd alloy: a sensitive electrochemical sensor for dopamine. Microchim Acta 185(8):397–406
16. Chen X, Liu Q, Liu M, Zhang X, Lin S, Chen Y, Zhuang J, Yang DP (2018) Protein-templated Fe_2O_3 microspheres for highly sensitive amperometric detection of dopamine. Microchim Acta 185(7): 340–348
17. Qin C, Bai X, Zhang Y, Gao K (2018) Photoelectrochemical CdSe/TiO_2 nanotube array microsensor for high-resolution in-situ detection of dopamine. Microchim Acta 185(5):278–286
18. Zhou Z, Sigdel S, Gong J, Vaagensmith B, Elbohy H, Yang H, Krishnan S, Wu XF, Qiao Q (2016) Graphene-beaded carbon nanofibers with incorporated Ni nanoparticles as efficient counter-electrode for dye-sensitized solar cells. Nano Energy 22:558–563
19. Wu Y, Ran F (2017) Vanadium nitride quantum dot/nitrogen-doped microporous carbon nanofibers electrode for high-performance supercapacitors. J Power Sources 344:1–10
20. Na L, Shao C, Li X, Miao F, Wang K, Liu Y (2016) CuO nanoparticles/nitrogen-doped carbon nanofibers modified glassy carbon electrodes for non-enzymatic glucose sensors with improved sensitivity. Ceram Int 42:11285–11293
21. Mamun KAA, Islam SK, Hensley DK, Mcfarlane N (2016) A glucose biosensor using CMOS potentiostat and vertically aligned carbon nanofibers. IEEE Trans Biomed Circuits Syst 10:807–816
22. Park J, Eun C (2016) Electrochemical behavior and determination of salicylic acid at carbon-fiber electrodes. Electrochim Acta 194: 346–356
23. Yoon J, Lee T, Bharate BG, Jo J, Oh BK, Choi JW (2016) Electrochemical H_2O_2 biosensor composed of myoglobin on MoS_2 nanoparticle-graphene oxide hybrid structure. Biosens Bioelectron 93:14–20
24. Parlak O, İncel A, Uzun L, Turner APF, Tiwari A (2017) Structuring Au nanoparticles on two-dimensional MoS_2 nanosheets for electrochemical glucose biosensors. Biosens Bioelectron 89:545–550
25. Kalantar-Zadeh K, Ou JZ (2015) Biosensors based on two-dimensional MoS_2. ACS Sensors 1:5–16
26. Kenry Geldert A, Zhang X, Zhang H, Lim CT (2016) Highly sensitive and selective aptamer-based fluorescence detection of a malarial biomarker using single-layer MoS2 nanosheets. ACS Sensors 1(11):1315–1321
27. Kıranşan KD, Topçu E (2018) Free-standing and flexible MoS_2/rGO paper electrode for amperometric detection of folic acid. Electroanalysis 30:810–818
28. Su S, Lu Z, Li J, Hao Q, Liu W, Zhu C, Shen X, Shi J, Wang L (2018) MoS_2-Au@Pt nanohybrid as a sensing platform for electrochemical nonenzymatic glucose detection. New J Chem 42: 6750–6755
29. Wang WQ, Yue HY, Yu ZM et al (2018) Synthesis of graphene/carbon nanofiber for electrochemical determination of levodopa in the presence of uric acid. Ionics 1:10–19
30. Yue HY, Huang S, Chang J, Heo C, Yao F, Adhikari S, Gunes F, Liu LC, Lee TH, Oh ES, Li B, Zhang JJ, Huy TQ, Luan NV, Lee YH (2014) ZnO nanowire arrays on 3D hierachical graphene foam: biomarker detection of Parkinson's disease. ACS Nano 8(2): 1639–1646
31. Yi SY, Lee JH, Hong HG (2014) A selective determination of levodopa in the presence of ascorbic acid and uric acid using a glassy carbon electrode modified with reduced graphene oxide. J Appl Electrochem 44:589–597
32. Huang Y, Tan Y, Feng C, Wang S, Wu H, Zhang G (2019) Synthesis of CuO/gC_3N_4 composites, and their application to voltammetric sensing of glucose and dopamine. Microchim Acta 186(1):10–19
33. Li Y, Jiang Y, Song Y, Li Y, Li S (2018) Simultaneous determination of dopamine and uric acid in the presence of ascorbic acid using a gold electrode modified with carboxylated graphene and silver nanocube functionalized polydopamine nanospheres. Microchim Acta 185(8):382–391

34. Zhuang X, Chen D, Zhang S, Luan F, Chen L (2018) Reduced graphene oxide functionalized with a CoS_2/ionic liquid composite and decorated with gold nanoparticles for voltammetric sensing of dopamine. Microchim Acta 185(3):166–174
35. Tang J, Jiang S, Liu Y, Zheng S, Bai L, Guo J, Wang J (2018) Electrochemical determination of dopamine and uric acid using a glassy carbon electrode modified with a composite consisting of a Co (II)-based metalorganic framework (ZIF-67) and graphene oxide. Microchim Acta 185(10):486–497
36. Chen D, Tian C, Li X, Li Z, Han Z, Zhai C, Quan Y, Cui R, Zhang G (2018) Electrochemical determination of dopamine using a glassy carbon electrode modified with a nanocomposite consisting of nanoporous platinum-yttrium and graphene. Microchim Acta 185(2):98–105
37. Khan MZH, Liu X, Tang Y, Zhu J, Hu W, Liu X (2018) A glassy carbon electrode modified with a composite consisting of gold nanoparticle, reduced graphene oxide and poly(L-arginine) for simultaneous voltammetric determination of dopamine, serotonin and L-tryptophan. Microchim Acta 185(9):439–449
38. Sáenz HSC, Hernández-Saravia LP, Selva JS, Sukeri A, Espinoza-Montero PJ, Bertotti M (2018) Electrochemical dopamine sensor using a nanoporous gold microelectrode: a proof-of-concept study for the detection of dopamine release by scanning electrochemical microscopy. Microchim Acta 185(8):367–376
39. Tavakolian E, Tashkhourian J (2018) Sonication-assisted preparation of a nanocomposite consisting of reduced graphene oxide and CdSe quantum dots, and its application to simultaneous voltammetric determination of ascorbic acid, dopamine and uric acid. Microchim Acta 185(10):456–464